Hyperpolarized NMR Metabolomics at Natural 13 C Abundance

Arnab Dey, Benoit Charrier, Estelle Martineau, Catherine Deborde, Elodie Gandriau, Annick Moing, Daniel Jacob, Dmitry Eshchenko, Marc Schnell, Roberto Melzi, et al.

analytical chemistry

pubs.acs.org/ac

Letter

Hyperpolarized NMR Metabolomics at Natural ^{13}C Abundance

Arnab Dey, Benoît Charrier, Estelle Martineau, Catherine Deborde, Elodie Gandriau, Annick Moing, Daniel Jacob, Dmitry Eshchenko, Marc Schnell, Roberto Melzi, Dennis Kurzbach, Morgan Ceillier, Quentin Chappuis, Samuel F. Cousin, James G. Kempf, Sami Jannin, Jean-Nicolas Dumez, and Patrick Giraudeau*

Cite This: *Anal. Chem.* 2020, 92, 14867−14871

Read Online

ACCESS | Metrics & More | Article Recommendations | Supporting Information

ABSTRACT: Metabolomics plays a pivotal role in systems biology, and NMR is a central tool with high precision and exceptional resolution of chemical information. Most NMR metabolomic studies are based on ^{1}H 1D spectroscopy, severely limited by peak overlap. ^{13}C NMR benefits from a larger signal dispersion but is barely used in metabolomics due to ca. 6000-fold lower sensitivity. We introduce a new approach, based on hyperpolarized ^{13}C NMR at natural abundance, that circumvents this limitation. A new untargeted NMR-based metabolomic workflow based on dissolution dynamic nuclear polarization (d-DNP) for the first time enabled hyperpolarized natural abundance ^{13}C metabolomics. Statistical analysis of resulting hyperpolarized ^{13}C data distinguishes two groups of plant (tomato) extracts and highlights biomarkers, in full agreement with previous results on the same biological model. We also optimize parameters of the semiautomated d-DNP system suitable for high-throughput studies.

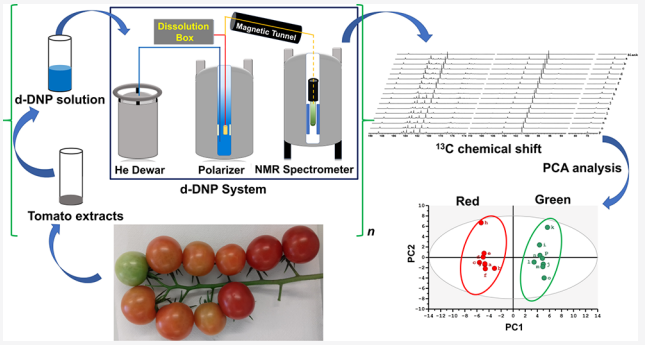

Metabolomic studies in systems biology elucidate the impacts of genetic alteration, disease, and environmental factors in broad fields such as precision medicine,[1] food,[2] plant,[3,4] or environmental sciences.[5] Untargeted metabolomics is of particular importance since it identifies crucial biomarkers without any *a priori* knowledge of the corresponding biological condition.[6] Mass spectrometry (MS) is widely used for untargeted analysis since it benefits from a much better sensitivity, typically 3 orders of magnitude, than NMR.[7] However, NMR can outperform MS in terms of reproducibility and repeatability needed to identify, with the highest achievable precision, the relative variations between metabolite concentrations from subtly distinct sample groups.[8] NMR metabolomics is therefore widely used for metabolomics applications across clinical and preclinical studies,[9,10] microbiology,[11] forensics,[12] and food[2] and plant sciences.[3,4] The vast majority of NMR metabolomics studies rely on one-dimensional (1D) ^{1}H spectra, as it is by far the most sensitive NMR approach.[3] However, ^{1}H NMR suffers from limited spectral resolution, often obscuring otherwise valuable data. ^{13}C NMR offers an appealing alternative thanks to broad ^{13}C chemical-shift dispersion (~200 vs ~10 ppm for ^{1}H) combined with relatively narrow spectral lines.[11] Moreover, ^{13}C is present in all metabolites (1.1% nat. ab.) with corresponding spectral diversity to identify, distinguish, and structurally characterize biomarkers. These advantages are long recognized[13,14] but thus far limited in application due to a roughly 5880-fold sensitivity disadvantage of ^{13}C (owing to its low natural abundance and gyromagnetic ratio) versus ^{1}H. Selective improvement of sensitivity with ^{13}C-enriched tracers[15] yields ~100 times better sensitivity but limits focus to specific metabolic pathways. Furthermore, resulting spectra can be complicated by undesired $^{13}C-^{13}C$ couplings (J_{CC}).

Hyperpolarization methods[16,17] can solve these issues by providing nonequilibrium ^{13}C polarization at greater than 10 000 times sensitivity gain for natural abundance carbon sites. Dissolution-dynamic nuclear polarization (d-DNP)[18−21] using ^{1}H DNP combined with $^{1}H \rightarrow {}^{13}C$ cross-polarization (CP)[22,23] is particularly promising owing to its ability to polarize ^{13}C spins in a nonselective fashion.[24] d-DNP hyperpolarizes solutes in frozen samples by transferring spin polarization from electrons of cosolvated radicals to nuclear spins. DNP occurs at cryogenic temperatures (1−4 K), followed by rapid dissolution with hot solvent and transfer of the hyperpolarized sample to an adjacent liquid-state, room-

Received: August 18, 2020
Accepted: October 15, 2020
Published: November 2, 2020

https://dx.doi.org/10.1021/acs.analchem.0c03510
Anal. Chem. 2020, 92, 14867−14871

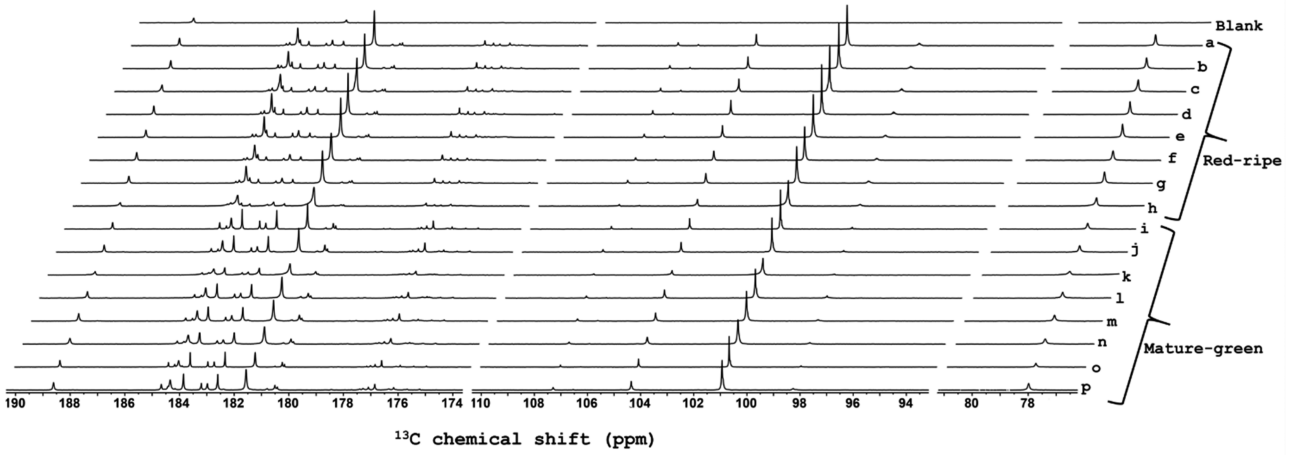

Figure 1. Stacked plot of d-DNP-enhanced single-scan ^{13}C NMR spectra of 16 tomato samples. At right, labels "a" to "h" refer to spectra of red−ripe fruit extracts, and "i" to "p" refer to mature−green fruit extracts. Selections from 76−82, 94−110, and 174−190 ppm are shown to focus on spectrally populated regions (full spectrum in Figure S7). The sample for the blank control spectrum (top) has signals only from Na-TSP-d_4 (188.6 ppm) and EDTA·Na_2·$2H_2O$ (182.9 ppm).

temperature NMR spectrometer. Dissolution and transfer do introduce some selectivity via variable losses from ^{13}C spin relaxation.[18−21]

The greater than 10 000 times enhancement from d-DNP was first demonstrated in 2003[18] and has evolved into a general and widely used hyperpolarization method in bioanalytical chemistry.[20] Nonetheless, as yet, there are only a limited number of applications to metabolomics.[25−27] Lerche et al. introduced a d-DNP ^{13}C approach to quantify metabolites in cancer cell extracts incubated with ^{13}C-enriched glucose.[25,26] While this took advantage of improved sensitivity from d-DNP and ^{13}C enrichment, this focused approach used isotopically labeled feed material. Untargeted, natural abundance methods remain unexplored by d-DNP.

In 2015, we reported a preliminary investigation of d-DNP assisted by cross-polarization (CP) for ^{13}C NMR of natural abundance metabolic extracts.[28] This enabled single-scan hyperpolarized ^{13}C NMR on quaternary carbons in about 30 min per sample. In contrast, classical high-field NMR without hyperpolarization required ∼12 h to produce ^{13}C spectra with significantly sparser peaks. In a later report, repeatability better than 4% (an essential condition for metabolomics) was demonstrated on a home-built d-DNP polarizer.[29] Here, we introduce a complete untargeted metabolomics approach for d-DNP NMR with real bioextracts at natural ^{13}C abundance. It consists of sample preparation, d-DNP hyperpolarization and conversion to a solution state, data processing, and statistical analysis, ultimately highlighting the variability between sample groups and identifying putative biomarkers. The test system consists of two groups of tomato fruit extracts at ripening stages of mature−green and red−ripe. For each stage, eight extracts were prepared from a single pooled sample of fruit powder, and their pH was adjusted. Thus, concentration, pH, and spin relaxation are uniform within one of the two groups, and intragroup observational differences highlight analytical variability only.

Samples were dissolved and flash-frozen in a glass-forming DNP solution with TEMPOL as a polarizing agent (see SI), then polarized for 11 min at 1.18 K with frequency-modulated[30] microwave irradiation and microwave-gated[31] cross-polarization (Figure S1). Hyperpolarized liquid-state spectra were acquired 12.8 s after initiation of dissolution, allowing time for fluid transfer and stabilization to a 400 MHz spectrometer equipped with a cryogenic probe. Figure S2a gives the pulse sequence for ^{13}C acquisition in a liquid state. Figure 1 shows resulting spectra, focused on the quaternary carbon regions, the hyperpolarization of which most readily survives the sample transfer due to relatively long $T_1(^{13}C)$. General application remains promising as most metabolites contain at least one quaternary carbon. Faster transfer times (<2 s) have been demonstrated that can enable extension to arbitrary carbon sites (e.g., methyl carbons).[32,33] Nonetheless, quaternary sites are quite sufficient to define small variations among biological states. On the basis of the reasonable assumption that the individual T_1 values are the same in all samples, hyperpolarized signals reflect the variations of analyte concentration between samples, but absolute concentration is inaccessible. Note that, even hyperpolarized, ^{13}C sensitivity at natural abundance is insufficient to quantify enhancements (i.e., the thermal signals are too weak) or to estimate T_1 values. Nonetheless, we typically observe 30,000 times more concentrated or ^{13}C-enriched samples, and $T_1 \sim 50-60$ s for quaternary sites.

The overall experiment duration (30 min from sample loading, through hyperpolarization, dissolution, and observation) is fully compatible with high-throughput metabolomics. In addition, the ^{13}C-hyperpolarized spectra can be processed through automated spectra and data analysis methods for conventional metabolomics. Spectra were processed as described in the SI, then divided into user-defined spectral regions ("buckets") (Figure S3), whose integral values were normalized with respect to that of sodium 3-trimethylsilylpropionate-d_4 (Na-TSP-d_4) (internal reference) at 188.6 ppm and to the weight of the fruit tissue powder. Then, as in standard NMR metabolomics, principal component analysis (PCA) was applied to the normalized set of ^{13}C integrals from each sample in order to distinguish biological variability.[34,35] Relevant details of the widely accepted PCA method are given in the SI. Figure 2 shows the resulting scores plot, where each point represents a single sample, the coordinates of which are determined by the collective contributions of all corresponding bucket integrals (weighed with the PCA "loadings" values). Point proximity indicates sample similarity, whereas group separation shows clear discrimination along the first-principal

https://dx.doi.org/10.1021/acs.analchem.0c03510
Anal. Chem. 2020, 92, 14867−14871

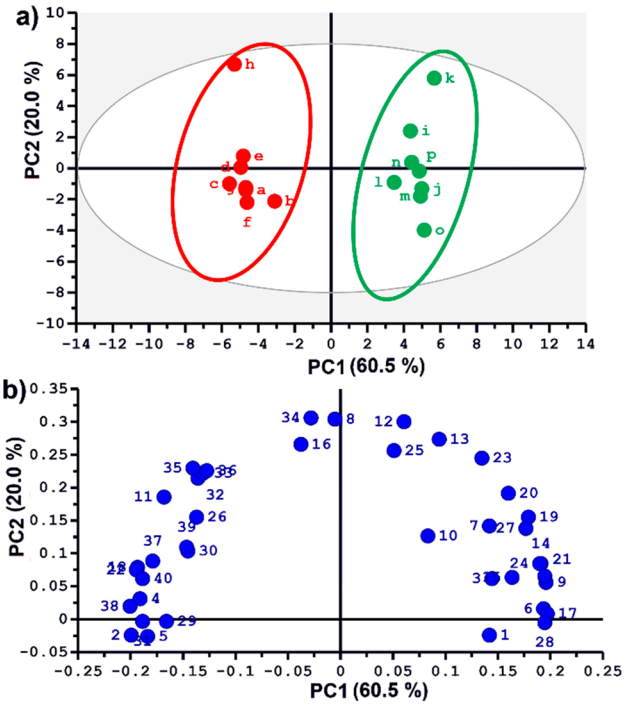

Figure 2. (a) Scores plot and (b) loadings plot of the principal component analysis (PCA) obtained from 40 spectral buckets from hyperpolarized ^{13}C spectra of 16 tomato fruit extracts. Integrals were normalized to Na-TSP-d_4 as an internal reference and to the weight of the sample used for extraction. Mean centering and unit variance scaling were used in PCA. Correspondence of bucket numbers to spectral regions is given in Figure S3.

component (PC1) for mature−green and red−ripe tomato fruit extracts. This reflects the robustness of the entire analytical workflow, including the complexities of d-DNP, since biological variability within each of the groups is not expected, as all red−ripe fruit samples were prepared from the same source and likewise for mature−green. The unexpected intragroup deviations (termed as "analytical" variability) of samples "h" (red) and "k" (green) along the PC2 axis results from the two times poorer line shape of spectra "h" and "k" (Figure 1). Still, the deviations on PC2, that makes a relatively modest 20.0% contribution to total variance, are not critical, as PC1 is the dominant component (explaining 60.5% of total variance).

To identify the key metabolites that differentiate the ripening stages, the PCA scores plot (Figure 2a) was compared to the loadings plot (Figure 2b), which scores relative contributions of individual spectral buckets to PC1 and PC2 constructions. Key metabolites were identified thanks to previously acquired spectra of individual commercial metabolites.

Resulting assignment and red/green fruit association of metabolites are given in Table S1. This succeeds in revealing expected patterns, such as higher content of some amino acids (aspartic acid, asparagine, glutamine, leucine, and threonine) and malic acid in tomato green fruit extracts, whereas sugars (sucrose and fructose), citric acid, and glutamic acid have higher contents in tomato red fruit extracts. These are in global agreement with known features of tomato metabolism[36] and for the first time shows the ability of hyperpolarized ^{13}C metabolomics to provide reliable biological discrimination. Furthermore, univariate analysis of the discriminant buckets (box plots in Figure S4, Kruskal−Wallis, $p < 0.05$) highlights the high quality of the discrimination. Overall, our approach establishes a complete, robust workflow for hyperpolarized, ^{13}C NMR-based metabolomic studies. Although the many assigned signals offer special benefits for metabolite identification, unidentified buckets also highlight a new promise of the hyperpolarized approach. Corresponding signals would not be observable by a thermally polarized approach, even with hours of signal-averaged acquisition.[18] Thus, d-DNP-enhanced NMR opens a window to previously inaccessible metabolites. Future avenues to assign such signals may utilize the combination of d-DNP with heteronuclear ultrafast 2D NMR.[37]

In contrast to prior hyperpolarized ^{13}C mixture analysis proof-of-concept papers,[28,29] our workflow utilized a more streamlined d-DNP system, where a single person can perform the key dissolution steps. This, along with high robustness and repeatable usage (for the present 16 samples, plus several tens of experiments performed before and since), is in favor of a broader, general use of our method. The robustness and repeatability are impressive given the variety of (reusable) sample-handling components required for a d-DNP process involving steps at less than 1.5 K and room temperature and a superheated solvent to drive conversion and transfer between these conditions.

Key experimental optimizations enabled such performance. The first consisted of optimizing the line shape of hyperpolarized ^{13}C signals to ensure well-resolved signals from ^{13}C metabolites. We found that microbubbles from rapid (1−2 s) injection of dissolution output to a 5 mm NMR tube were responsible for initial broad, asymmetric line shapes. In order to avoid bubbles, we decreased the surface tension on the walls of the NMR tubes by precleaning with an alkaline solution (Hellmanex). Figure S5 shows the improvement of line shape and spectral resolution after this treatment. This also translates to 3 times better ^{13}C sensitivity (Figure S6), since it enables a much shorter postdissolution delay to reach settled conditions and optimal S/N that balances lost ^{13}C hyperpolarization during the transfer against initial intensity build-up as spectral lines narrow with homogenization (e.g., bubble dissipation) in the NMR sample.

Analytical metabolomics demands that variability is dominated by biological inputs, with insignificant (or small) contributions from the experimental method. Using the above treatment and timing optimizations, we demonstrate the needed precision in Figure 3. Progressive improvements in repeatability are shown for a series in which postdissolution timing of NMR observation was separately optimized for three protocols: A (ethanol-cleaned NMR tube, with 22.8 s delay to acquisition), B (Hellmanex treatment, with 12.8 s delay), and C (case B plus normalization of integrals according to the Na-TSP-d_4 internal reference). Hellmanex alone provided 3%−5% drops in CV among metabolites in the sample (pyruvate, acetate, and alanine), and the internal reference yielded further 3%−9% drops for ultimate CV values of 2.0%, 4.8%, and 4.1% for the respective compounds. The improvements reflect both more reliable attainment of suitable conditions for solution-state NMR and the natural benefits of noted 3 times higher S/N.

In summary, we demonstrate that hyperpolarized, natural abundance ^{13}C NMR is suitable for analytical metabolomics on relevant biological samples. This greatly expands the impact of NMR in the metabolomic field. This hyperpolarized ^{13}C approach is complementary to valuable and more established

https://dx.doi.org/10.1021/acs.analchem.0c03510
Anal. Chem. 2020, 92, 14867−14871

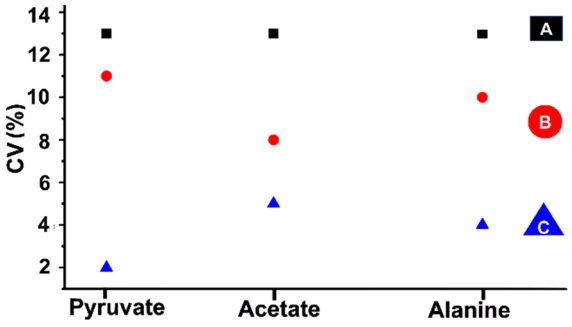

Figure 3. Coefficient of variation (CV (%)) of d-DNP enhanced ^{13}C signal integrals (based on five successive experiments) for a standard metabolite mixture (pyruvate, acetate, alanine) at natural abundance using three experimental protocols (A, B, C). Solution-state spectra were detected with a 90° flip angle, after a postdissolution delay that ensured an optimum signal-to-noise ratio (S/N) for each case A, B, and C. CV at "A" was obtained using ethanol-washed NMR tubes, yielding optimum S/N at 22.8 s after dissolution. CV at "B" was obtained using NMR tubes additionally treated with Hellmanex (procedure in SI), yielding S/N optimum at 12.8 s after dissolution. CV at "C" was achieved under similar conditions as "B" but normalizing all signal integrals using the Na-TSP-d_4 internal reference as described in the text.

^{1}H NMR methods for metabolomics. Indeed, ^{1}H methods can be limited by spectral resolution and sensitivity issues, sometimes failing to clarify biochemical fingerprints or to pinpoint metabolic markers of functional states. For ^{13}C NMR, only hyperpolarization can practically open a new window to the field. We have proven the needed precision, accuracy, and throughput using the sophisticated, but ultimately straightforward, approach of d-DNP. This success motivates both the broader adoption of natural abundance ^{13}C metabolomics with application to challenging biological problems and the development of d-DNP instrumentation for the full community. Our work highlights development areas to further extend the value of NMR in metabolomics, including reduction of the time from dissolution to NMR observation to less than 5 s. Correspondingly lower hyperpolarization losses should enable analytical ^{1}H metabolomics, as well as access to greater chemical functionality with natural abundance ^{13}C. On the technical side, progresses are expected to make the experiment much less expensive, in particular, through the design of cryogen consumption-free systems that will undoubtedly broaden the application scope of hyperpolarized metabolomics.[38,39]

■ ASSOCIATED CONTENT

Supporting Information

The Supporting Information is available free of charge at https://pubs.acs.org/doi/10.1021/acs.analchem.0c03510.

Experimental details, procedure of Hellmanex treatment, and figures and tables (PDF)

■ AUTHOR INFORMATION

Corresponding Author

Patrick Giraudeau − *Université de Nantes, CNRS, CEISAM UMR 6230, F-44000 Nantes, France;* orcid.org/0000-0001-9346-9147; Email: patrick.giraudeau@univ-nantes.fr

Authors

Arnab Dey − *Université de Nantes, CNRS, CEISAM UMR 6230, F-44000 Nantes, France*

Benoît Charrier − *Université de Nantes, CNRS, CEISAM UMR 6230, F-44000 Nantes, France*

Estelle Martineau − *Université de Nantes, CNRS, CEISAM UMR 6230, F-44000 Nantes, France; SpectroMaitrise, CAPACITES SAS, F-44000 Nantes, France*

Catherine Deborde − *INRAE, Univ. Bordeaux, UMR Biologie du Fruit et Pathologie and Bordeaux Metabolome, MetaboHUB, Centre INRAE de Nouvelle Aquitaine-Bordeaux, F-33140 Villenave d'Ornon, France*

Elodie Gandriau − *Université de Nantes, CNRS, CEISAM UMR 6230, F-44000 Nantes, France*

Annick Moing − *INRAE, Univ. Bordeaux, UMR Biologie du Fruit et Pathologie and Bordeaux Metabolome, MetaboHUB, Centre INRAE de Nouvelle Aquitaine-Bordeaux, F-33140 Villenave d'Ornon, France*

Daniel Jacob − *INRAE, Univ. Bordeaux, UMR Biologie du Fruit et Pathologie and Bordeaux Metabolome, MetaboHUB, Centre INRAE de Nouvelle Aquitaine-Bordeaux, F-33140 Villenave d'Ornon, France*

Dmitry Eshchenko − *Bruker Biospin, 8117 Fällanden, Switzerland*

Marc Schnell − *Bruker Biospin, 8117 Fällanden, Switzerland*

Roberto Melzi − *Bruker Italia Srl, 20158 Milano, Italy*

Dennis Kurzbach − *University of Vienna, Faculty of Chemistry, Institute of Biological Chemistry, 1090 Vienna, Austria;* orcid.org/0000-0001-6455-2136

Morgan Ceillier − *Université de Lyon, CNRS, Université Claude Bernard Lyon 1, F-69100 Villeurbanne, France*

Quentin Chappuis − *Université de Lyon, CNRS, Université Claude Bernard Lyon 1, F-69100 Villeurbanne, France*

Samuel F. Cousin − *Université de Lyon, CNRS, Université Claude Bernard Lyon 1, F-69100 Villeurbanne, France*

James G. Kempf − *Bruker Biospin, Billerica, Massachusetts 01821, United States*

Sami Jannin − *Université de Lyon, CNRS, Université Claude Bernard Lyon 1, F-69100 Villeurbanne, France*

Jean-Nicolas Dumez − *Université de Nantes, CNRS, CEISAM UMR 6230, F-44000 Nantes, France;* orcid.org/0000-0002-5394-8001

Complete contact information is available at: https://pubs.acs.org/10.1021/acs.analchem.0c03510

Notes

The authors declare the following competing financial interest(s): D.E., M.S., R.M., and J.G.K. are employees of Bruker Biospin, which supplied the d-DNP polarizer. It is not a commercial instrument but a step in ongoing Bruker R&D.

■ ACKNOWLEDGMENTS

The authors acknowledge funding from the European Research Council under the European Union's Horizon 2020 research and innovation program (ERC Grant Agreements n° 814747/SUMMIT, DINAMIX n° 801774, n° 714519/HP4all, HYPROTIN n° 801936), support from Bruker BioSpin, the Corsaire metabolomics platform, and from MetaboHUB (ANR-11-INBS-0010). The authors acknowledge Isabelle Atienza for taking care of the tomato plants and kind assistance during d-DNP experiments from Corentin Jacquemmoz, Virginie Silvestre, Achille Marchand, and Ritu Raj Mishra.

https://dx.doi.org/10.1021/acs.analchem.0c03510
Anal. Chem. 2020, 92, 14867−14871

REFERENCES

(1) Puchades-Carrasco, L.; Pineda-Lucena, A. *Curr. Top. Med. Chem.* **2017**, *17* (24), 2740−2751.
(2) Petrakis, E. A.; Cagliani, L. R.; Polissiou, M. G.; Consonni, R. *Food Chem.* **2015**, *173*, 890−896.
(3) Freitas, D. d. S.; Carlos, E. F.; Gil, M. C. S. d. S.; Vieira, L. G. E.; Alcantara, G. B. *J. Agric. Food Chem.* **2015**, *63*, 7582−7588.
(4) Allwood, J. W.; De Vos, R. C.; Moing, A.; Deborde, C.; Erban, A.; Kopka, J.; Goodacre, R.; Hall, R. D. *Methods Enzymol.* **2011**, *500*, 299−336.
(5) Viant, M. R. *Metabolomics* **2009**, *5*, 1−2.
(6) Gertsman, I.; Barshop, B. A. *J. Inherited Metab. Dis.* **2018**, *41*, 355−366.
(7) Ren, J.-L.; Zhang, A.-H.; Kong, L.; Wang, X.-J. *RSC Adv.* **2018**, *8*, 22335−22350.
(8) Bingol, K.; Brüschweiler, R. *Curr. Opin. Clin. Nutr. Metab. Care* **2015**, *18*, 471−477.
(9) Kim, E. R.; Kwon, H. N.; Nam, H.; Kim, J. J.; Park, S.; Kim, Y.-H. *Sci. Rep.* **2019**, *9*, 1−10.
(10) Bertini, I.; Calabrò, A.; De Carli, V.; Luchinat, C.; Nepi, S.; Porfirio, B.; Renzi, D.; Saccenti, E.; Tenori, L. *Journal of Proteome Research.* **2009**, *8*, 170−177.
(11) Palama, T. L.; Canard, I.; Rautureau, G. J. P.; Mirande, C.; Chatellier, S.; Elena-Herrmann, B. *Analyst* **2016**, *141*, 4558−4561.
(12) Castillo-Peinado, L. S.; Luque de Castro, M. D. *Anal. Chim. Acta* **2016**, *925*, 1−15.
(13) Clendinen, C. S.; Lee-McMullen, B.; Williams, C. M.; Stupp, G. S.; Vandenborne, K.; Hahn, D. A.; Walter, G. A.; Edison, A. S. *Anal. Chem.* **2014**, *86*, 9242−9250.
(14) Dayrit, F. M.; Dios, A. C. d. *Intech* **2017**, 81−103.
(15) Clendinen, C. S.; Stupp, G. S.; Ajredini, R.; Lee-McMullen, B.; Beecher, C.; Edison, A. S. *Front. Plant Sci.* **2015**, *6*, 1−13.
(16) Kovtunov, K. V.; Pokochueva, E. V.; Salnikov, O. G.; Cousin, S. F.; Kurzbach, D.; Vuichoud, B.; Jannin, S.; Chekmenev, E. Y.; Goodson, B. M.; Barskiy, D. A.; Koptyug, I. V. *Chem. - Asian J.* **2018**, *13*, 1857−1871.
(17) Nikolaou, P.; Goodson, B. M.; Chekmenev, E. Y. *Chem. - Eur. J.* **2015**, *21*, 3156−3166.
(18) Ardenkjær-Larsen, J. H.; Fridlund, B.; Gram, A.; Hansson, G.; Hansson, L.; Lerche, M. H.; Servin, R.; Thaning, M.; Golman, K. *Proc. Natl. Acad. Sci. U. S. A.* **2003**, *100* (18), 10158−10163.
(19) Plainchont, B.; Berruyer, P.; Dumez, J.-N.; Jannin, S.; Giraudeau, P. *Anal. Chem.* **2018**, *90*, 3639−3650.
(20) Jannin, S.; Dumez, J.-N.; Giraudeau, P.; Kurzbach, D. *J. Magn. Reson.* **2019**, *305*, 41−50.
(21) Ardenkjær-Larsen, J. H. *J. Magn. Reson.* **2016**, *264*, 3−12.
(22) Bornet, A.; Melzi, R.; Perez Linde, A. J.; Hautle, P.; van den Brandt, B.; Jannin, S.; Bodenhausen, G. *J. Phys. Chem. Lett.* **2013**, *4*, 111−114.
(23) Jannin, S.; Bornet, A.; Melzi, R.; Bodenhausen, G. *Chem. Phys. Lett.* **2012**, *549*, 99−102.
(24) Vuichoud, B.; Milani, J.; Bornet, A.; Melzi, R.; Jannin, S.; Bodenhausen, G. *J. Phys. Chem. B* **2014**, *118*, 1411−1415.
(25) Lerche, M. H.; Yigit, D.; Frahm, A. B.; Ardenkjær-Larsen, J. H.; Malinowski, R. M.; Jensen, P. R. *Anal. Chem.* **2018**, *90*, 674−678.
(26) Frahm, A. B.; Jensen, P. R.; Ardenkjær-Larsen, J. H.; Yigit, D.; Lerche, M. H. *J. Magn. Reson.* **2020**, *316*, 106750.
(27) Zhang, G.; Ahola, S.; Lerche, M. H.; Telkki, V.-V.; Hilty, C. *Anal. Chem.* **2018**, *90*, 11131−11137.
(28) Dumez, J.-N.; Milani, J.; Vuichoud, B.; Bornet, A.; Lalande-Martin, J.; Tea, I.; Yon, M.; Maucourt, M.; Deborde, C.; Moing, A.; Frydman, L.; Bodenhausen, G.; Jannin, S.; Giraudeau, P. *Analyst* **2015**, *140*, 5860−5863.
(29) Bornet, A.; Maucourt, M.; Deborde, C.; Jacob, D.; Milani, J.; Vuichoud, B.; Ji, X.; Dumez, J. N.; Moing, A.; Bodenhausen, G.; Jannin, S.; Giraudeau, P. *Anal. Chem.* **2016**, *88*, 6179−6183.
(30) Bornet, A.; Milani, J.; Vuichoud, B.; Perez Linde, A. J.; Bodenhausen, G.; Jannin, S. *Chem. Phys. Lett.* **2014**, *602*, 63−67.
(31) Bornet, A.; Pinon, A.; Jhajharia, A.; Baudin, M.; Ji, X.; Emsley, L.; Bodenhausen, G.; Ardenkjær-Larsen, J. H.; Jannin, S. *Phys. Chem. Chem. Phys.* **2016**, *18*, 30530−30535.
(32) Bowen, S.; Hilty, C. *Phys. Chem. Chem. Phys.* **2010**, *12*, 5766−5770.
(33) Chen, H. Y.; Hilty, C. *ChemPhysChem* **2015**, *16*, 2646−2652.
(34) Stoyanova, R.; Brown, T. R. *NMR Biomed.* **2001**, *14*, 271−277.
(35) Stoyanova, R.; Brown, T. R. *J. Magn. Reson.* **2002**, *154*, 163−75.
(36) Lemaire-Chamley, M.; Mounet, F.; Deborde, C.; Maucourt, M.; Jacob, D.; Moing, A. *Metabolites* **2019**, *9*, 93.
(37) Giraudeau, P.; Shrot, Y.; Frydman, L. *J. Am. Chem. Soc.* **2009**, *131*, 13902−13903.
(38) Baudin, M.; Vuichoud, B.; Bornet, A.; Bodenhausen, G.; Jannin, S. *J. Magn. Reson.* **2018**, *294*, 115−121.
(39) Ardenkjær-Larsen, J. H.; Bowen, S.; Petersen, J. R.; Rybalko, O.; Vinding, M. S.; Ullisch, M.; Nielsen, N. C. *Magn. Reson. Med.* **2019**, *81*, 2184−2194.

https://dx.doi.org/10.1021/acs.analchem.0c03510
Anal. Chem. 2020, 92, 14867−14871